



Account/Revue

Towards highly efficient, intelligent and bimodal imaging probes: Novel approaches provided by lanthanide coordination chemistry

Célia S. Bonnet, Éva Tóth*

Centre de biophysique moléculaire, CNRS, rue Charles-Sadron, 45071 Orléans, France

ARTICLE INFO

Article history:

Received 8 December 2009

Accepted after revision 25 March 2010

Available online 21 May 2010

Keywords:

Bioinorganic chemistry

Lanthanides

Ligand design

Magnetic properties

Imaging agents

Gadolinium

Mots clés :

Chimie bio-inorganique

Lanthanides

Conception de ligands

Propriétés magnétiques

Imagerie

Gadolinium

ABSTRACT

Gd³⁺ complexes are widely used as contrast enhancing agents in medical magnetic resonance imaging (MRI). In recent years, new fields have emerged in their development. The general tendency of using higher magnetic fields in biomedical and clinical MRI for a better signal to noise ratio calls for new contrast agents specifically optimized for such high field applications. Molecular imaging, aiming at the non-invasive visualisation of expression and function of bioactive molecules, requires imaging probes that provide a specific magnetic response to a particular molecular event. Finally, bimodal imaging may allow for combining the excellent resolution of MRI with a good sensitivity of other imaging modalities, such as optical methods. It requires bimodal imaging probes that satisfy requirements for both modalities within a single molecule. Here we review our latest efforts to develop novel lanthanide-based contrast agents in these specific fields and demonstrate the possibilities offered by lanthanide coordination chemistry.

© 2010 Académie des sciences. Published by Elsevier Masson SAS. All rights reserved.

R É S U M É

Les complexes de Gd³⁺ sont couramment utilisés en tant qu'agents de contraste pour l'imagerie par résonance magnétique nucléaire (IRM). Ces dernières années ont vu l'émergence de nouvelles directions de recherche. L'apparition d'imagers de champs magnétiques toujours plus élevés dans les domaines biomédical et clinique nécessite de créer des agents de contraste qui seront optimisés pour ces hauts champs. L'imagerie moléculaire est devenue un domaine incontournable. Elle consiste à visualiser de façon non-invasive, non plus l'anatomie, mais l'expression et la fonction de molécules actives biologiquement. Cela requiert le développement de sondes d'imagerie apportant une réponse magnétique spécifique à l'événement moléculaire visé. L'imagerie bimodale devrait permettre de combiner l'excellente résolution de l'IRM avec la bonne sensibilité d'autres techniques d'imagerie comme l'imagerie optique par exemple. Dans ce but, les sondes d'imagerie bimodales correspondantes doivent satisfaire les contraintes des deux modalités d'imagerie à l'aide d'une seule et même molécule. Dans cet article, nous passons en revue nos récents efforts pour développer de nouveaux agents de contraste à base de lanthanides dans ces domaines en essor et nous montrons comment la chimie de coordination des lanthanides se trouve au cœur de ces nouveaux développements.

© 2010 Académie des sciences. Publié par Elsevier Masson SAS. Tous droits réservés.

* Corresponding author.

E-mail address: eva.jakabtoth@cnrs-orleans.fr (É. Tóth).

1. Introduction

Since its introduction in the early 1980s, magnetic resonance imaging (MRI) has evolved into one of the most powerful imaging modalities in clinical diagnosis and biomedical research. MRI has many positive features: it is non-invasive, it has an exceptional temporal and spatial resolution (in contrast to PET), unlimited tissue penetration (in contrast to optical methods), and it does not involve ionizing radiation (in contrast to X-ray, SPECT or PET). Magnetic resonance images are based on proton density and proton relaxation dynamics, parameters which vary according to the tissue under examination and reflect its physical and chemical properties. In order to compensate the relatively low sensitivity of MRI, paramagnetic substances, in particular Gd^{3+} complexes are commonly used as contrast enhancing agents [1–4]. The role of contrast agents is to shorten the relaxation times of tissue water protons in their vicinity which results in an improved contrast of the images. In the clinical practice today, 30–40% of all images are recorded after administration of a contrast medium. Undoubtedly, the use of contrast agents has largely contributed to the spectacular evolution of MRI.

In parallel, the great success of Gd^{3+} complexes in MRI contrast agent applications has promoted intensive research on lanthanide complexes, and the last two decades have witnessed the renaissance of lanthanide coordination chemistry in aqueous solution [5–7]. Lanthanides are gaining importance in other biomedical applications as well, including both diagnosis [8] and therapy [9]. However, with over 200 million doses injected so far into patients, which represent 95% of all MRI contrast agent injections, Gd^{3+} -based magnetic resonance imaging contrast agents are the most widely used lanthanide complexes in medicine.

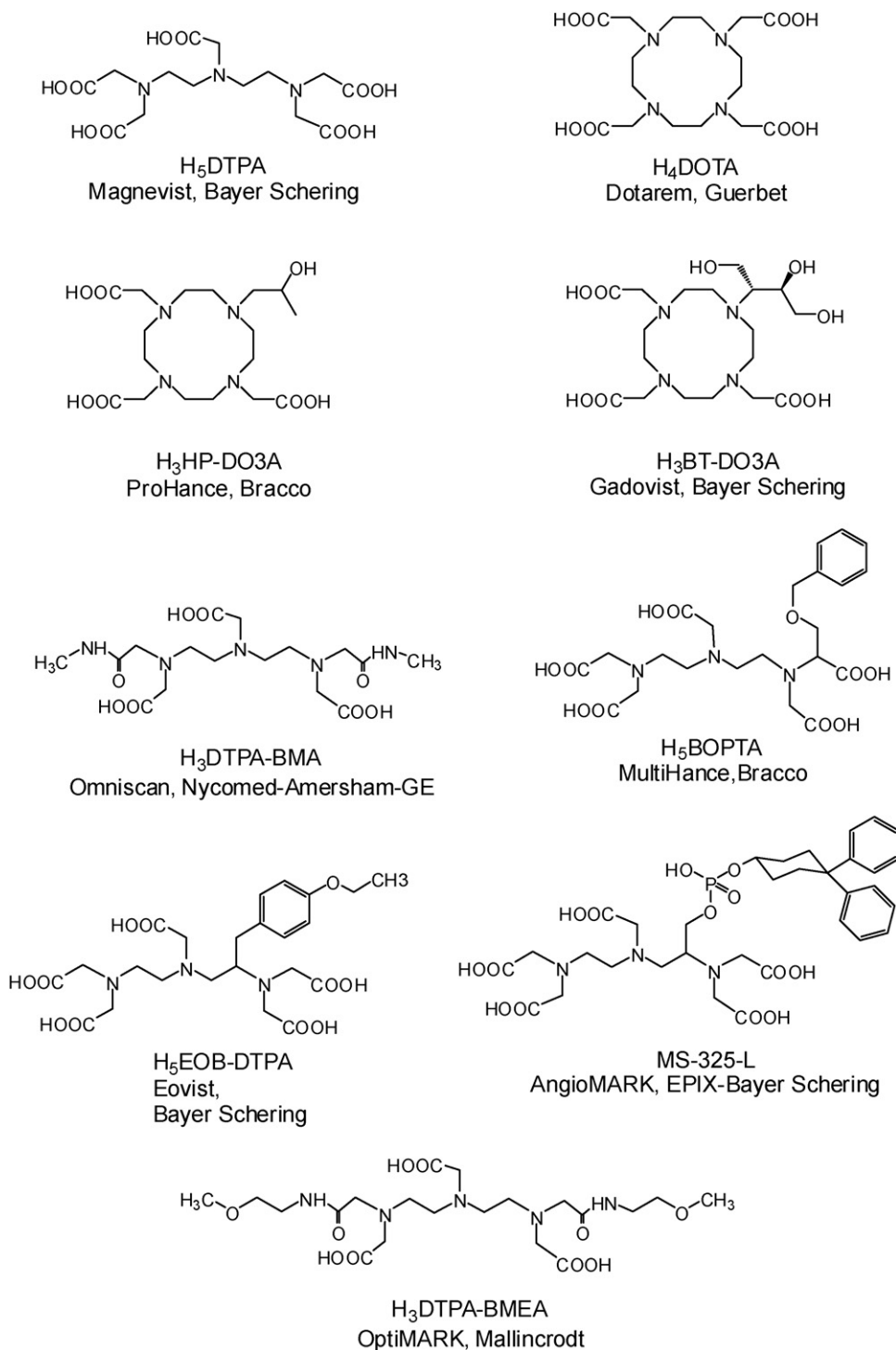
Given its seven unpaired electrons, Gd^{3+} is the most paramagnetic stable metal ion. This high paramagnetism and a relatively slow electronic relaxation, originating from its symmetric S -state, render the Gd^{3+} ion particularly efficient in reducing the nuclear relaxation times of the surrounding water protons, which is the basis of the contrast enhancing effect in MRI. The efficiency of a paramagnetic chelate to act as a contrast agent is most often expressed by its longitudinal proton relaxivity, r_1 , referring to the paramagnetic enhancement of the longitudinal relaxation rate, $1/T_1$, of bulk water protons by a unity concentration of the agent (1 mM). The free gadolinium ion, Gd^{3+} , induces toxicity in different ways and cannot be directly injected into the blood. Gd^{3+} has a tendency to form hydroxo complexes at physiological pH, it can also bind to proteins, replace other metal ions in enzymes, or, due to its similar size to Ca^{2+} (107.8 pm for Gd^{3+} vs. 114 pm for Ca^{2+}), it may interfere in Ca^{2+} -regulated signal transmission processes. In order to circumvent toxicity, Gd^{3+} is complexed with multidentate poly(aminocarboxylate) ligands, such as DTPA⁵⁻ or DOTA⁴⁻ or their derivatives, which are able to ensure a high thermodynamic stability and kinetic inertness of the complex (Scheme 1).

In the last years, considerable effort has been devoted to gain insight into the relationship between the structure and dynamics and the MRI contrast agent efficacy of Gd^{3+} complexes. This understanding has already resulted in the design of novel, more efficient potential agents; nevertheless, the optimization of the relaxation properties of Gd^{3+} complexes by rational ligand design remains an active research field. Recently, the chemistry efforts have followed the general tendency of technical MRI developments to go to high magnetic fields. This led to the development of specific contrast agents dedicated to high magnetic fields (> 3 Tesla), above the typical clinical field strengths used today. In the first part of the review, we will survey these high field agents.

Lately, a new area of imaging has emerged, called molecular imaging, which aims at the non-invasive visualisation of expression and function of bioactive molecules. Molecular imaging seeks for the detection of the biochemical or physiological abnormalities underlying the disease, rather than the structural consequences of these abnormalities as typically visualized by classical anatomical imaging. In contrast to anatomical imaging, molecular imaging always requires a molecular imaging probe which has to be specific to the particular molecular event that we want to detect. Consequently, chemistry has a pivotal role in the development of new molecular imaging approaches.

Among all molecular imaging modalities, MRI is particularly attractive. Its exceptional resolution allows acquiring anatomical images in conjunction with mapping the activity of biomarkers. Not less importantly, the richness of the chemistry of lanthanide complexes offers almost unlimited possibilities to develop MRI probes with a relaxivity response to various physicochemical parameters of tissues that might be related to disease processes and whose MRI mapping can be of great diagnostic value. The diversity of chemical modulation pathways offers invaluable tools for the development of intelligent, lanthanide-based MR imaging agents, which is not at all possible in the case of nuclear techniques where the signal is independent of the chemical nature of the imaging probe. In the second part of the review, we will discuss some recent examples of molecular imaging agents, such as calcium-sensitive or enzymatically activated probes.

In parallel to efforts in molecular imaging, a novel approach of combining different imaging modalities is gaining more interest primarily in biomedical research, but also in the clinics. Among the state-of-the-art bioimaging modalities, some are characterized by high resolution but low sensitivity (MRI), others by high sensitivity but low resolution (nuclear or optical imaging techniques). Bimodal/multimodal imaging offers the advantage of coupling the high sensitivity of one technique with the high resolution of another. Ideally, bimodal imaging probes integrate on the same molecular entity a reporter optimized for each of the imaging modes, with the benefits of simplified design, physical characterization and formulation of the probe, and single biodistribution, thus an overlap of the examinations by the two imaging modalities. Lanthanides are particularly well adapted for bimodal



Scheme 1. Ligand structures of the commercial, Gd-based MRI contrast agents.

design, since they have fundamentally different magnetic and optical properties, while being chemically similar, allowing the easy replacement of one by another. In the last part of the review, we show examples from the field of lanthanide-based bimodal (optical/MRI) contrast agents.

2. Gd-based MRI contrast agents for application at high magnetic field

In MRI, the amount of available signal is directly related to the static magnetic field strength. According to the

Boltzmann distribution, an increase in the field is accompanied by an accentuation of the difference between the populations of parallel and antiparallel spins. This yields an increase in the potential signal which varies with the square of the B_0 field, counterbalanced by a linear progression of the noise. As a result, the signal-to-noise ratio follows a linear relation with the value of the field: it is theoretically twice as high at 3.0 Tesla as at 1.5 Tesla. The improvement in the signal-to-noise ratio with increasing magnetic field then translates to an increased spatial and temporal resolution. In addition, T_1 relaxation times of grey and white matter also increase with field strength, thus at high field the uptake of a contrast agent will result in a more significant shortening of T_1 . This can allow for decreasing the contrast agent dose to generate the same contrast. Indeed, the image contrast was similar at 1.5 Tesla and at 3 Tesla using only a half-dose of GdDTPA²⁻ [10]. Until recently, common clinical scanners operated at less or equal to 1.5 Tesla. Today, 3 Tesla scanners are widely available in the clinics, and for experimental animal studies, much higher fields (≥ 9.4 Tesla; 400 MHz) become commonly used [11]. Since it is technically easier to increase the field if the diameter is small, high field magnets were primarily available for small animals. Nevertheless, high fields also enter human experimental studies; the first results on a human 9.4 Tesla (400 MHz) magnet were already published in 2006 [12] and in Neurospin, the French neuroscience research centre, an 11.7 Tesla magnet for whole body imaging is under construction [13].

The overall relaxation effect of a Gd³⁺ complex originates from three distinct mechanisms: the outer sphere mechanism (related to water molecules diffusing around the paramagnetic centre), the inner-sphere mechanism (arising from the water molecules directly bound to the Gd³⁺ and exchanging with the bulk) and the second sphere mechanism (concerning water molecules bound to the ligand by hydrogen bonding for example). The most efficient one is the inner-sphere term; moreover, this is the contribution which can be mostly modulated by chemical design. Through the inner-sphere term, the efficiency of a Gd³⁺ chelate is inherently related to its microscopic parameters, such as the water exchange, rotational dynamics or electronic relaxation (Fig. 1a). Others and we have been active in the optimization of water exchange [14–18] and rotational dynamics [19–21] with the objective of increasing relaxivity. The most spectacular results were achieved by slowing down the rotation of the chelates by using macromolecules, which lead to a remarkable relaxivity improvement at intermediate frequencies (20–60 MHz) as compared to commercial agents [7]. Above 60 MHz, however, r_1 of the macromolecular agents drops strongly with increasing magnetic field and, at high frequencies (above 100 MHz), their relaxivity is hardly superior to that of small Gd³⁺ chelates.

Given the linear proportionality between the inner-sphere contribution to relaxivity and the number of water molecules directly coordinated to the Gd³⁺ ion, the most straightforward way to increase relaxivity at any, including high frequencies, is to increase the hydration number. In this perspective, several bishydrated Gd³⁺ complexes have

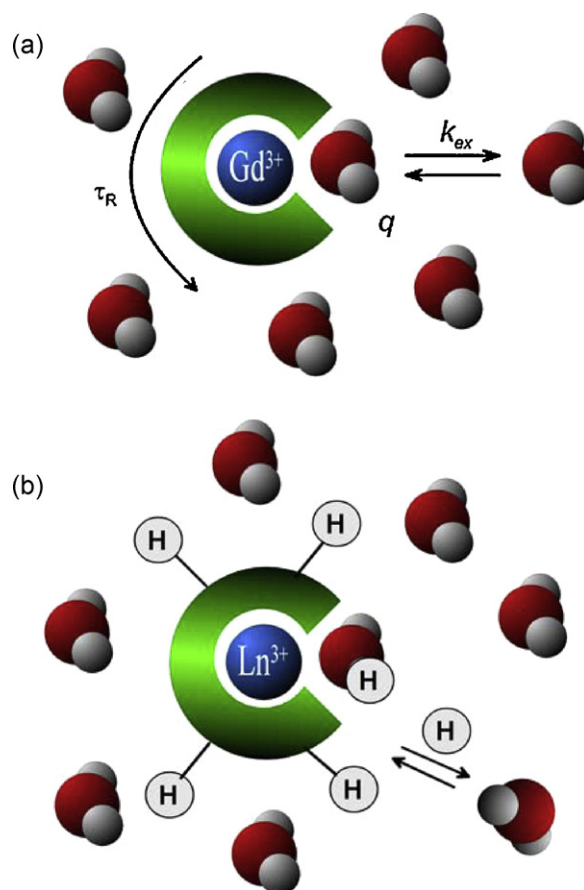
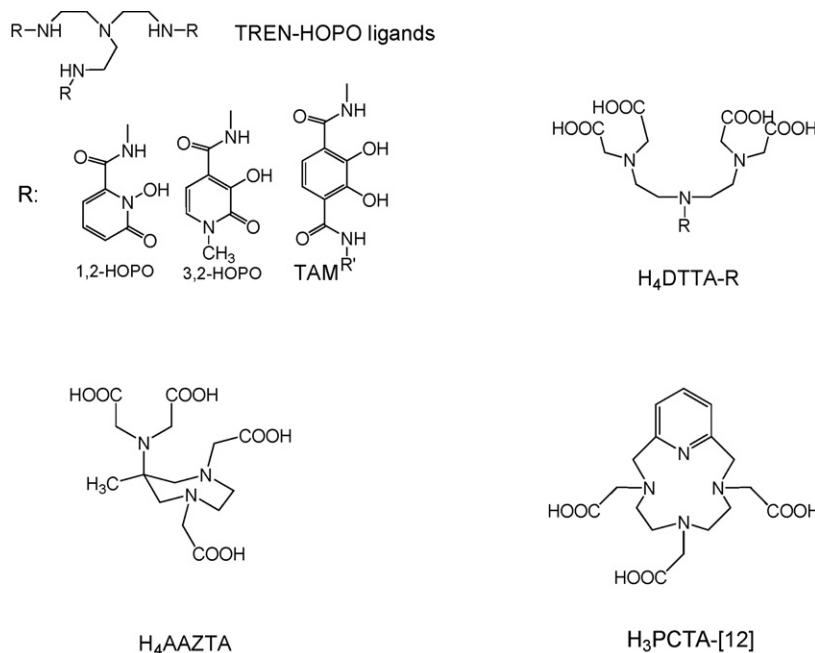


Fig. 1. a: the most important parameters influencing inner-sphere relaxivity of a Gd³⁺ complex: the number of water molecules directly coordinated to the Gd³⁺, q , the exchange rate of the inner-sphere water, k_{ex} , and the rotational motion of the complex, characterized by the rotational correlation time, τ_R ; b: lanthanide complexes as PARACEST agents: the PARACEST effect stems from proton exchange between the bulk water and protons on the ligand or on the coordinated water molecules.

been reported based on the HOPO family [22], on AAZTA [23], DTTA [24] or PCTA ligands [25] (Scheme 2). When using seven-coordinate ligands affording for two inner-sphere water molecules, however, one has to consider that increasing the hydration number should not be detrimental to the thermodynamic stability and kinetic inertness of the complex, which are the key parameters to ensure safe *in vivo* use. Another route to increase relaxivity especially at high field which does not influence thermodynamic stability of the complex is to use highly hydrophilic complexes which will display a large second sphere contribution to relaxivity. The success of this method has been demonstrated for a Gd-binding peptide [26]. Nevertheless, when designing a ligand, the prediction and rationalization of the second sphere relaxivity contribution remain difficult.

Apart from an increase in the hydration number, the optimisation of the relaxivity specifically for high magnetic field requires the fine-tuning of the microscopic parameters of the Gd³⁺ complex to optimal values which are



Scheme 2. Ligands affording bishydrated Gd³⁺ complexes.

different from those at intermediate fields. Namely, as the Solomon-Bloembergen-Morgan theory predicts, at proton Larmor frequencies above 200 MHz r_1 increases with the inverse rotational correlation time $1/\tau_R$, in contrast to lower frequencies, where it is proportional to τ_R (Fig. 2). Thus at high frequencies, intermediate-size, rigid molecules will be favoured over large ones, with an optimal τ_R of ~ 400 ps at 400 MHz (the exact value of the optimal

rotational correlation time will also be dependent on the other influencing parameters). It has to be noted that the optimal rotational correlation time is very sensitive to the magnetic field, but remains, nevertheless, in the range of 400–1000 ps. The optimal value of the water exchange rate will also be different, and considerably higher than that for current clinical fields [27]. The development of contrast agents specifically designed for high field applications is an

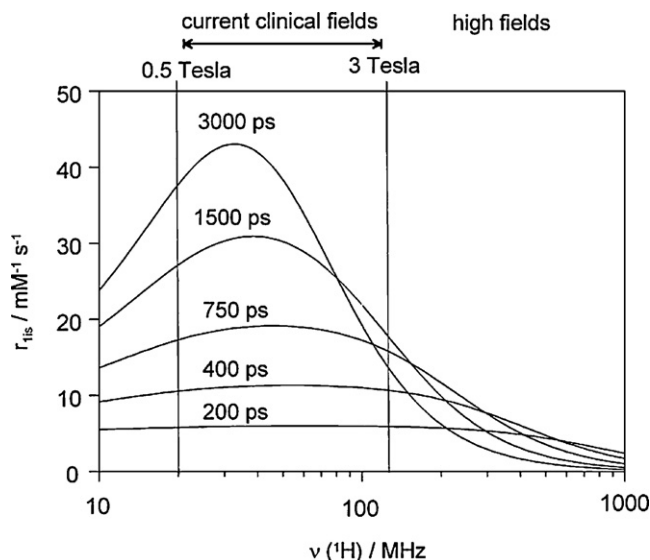
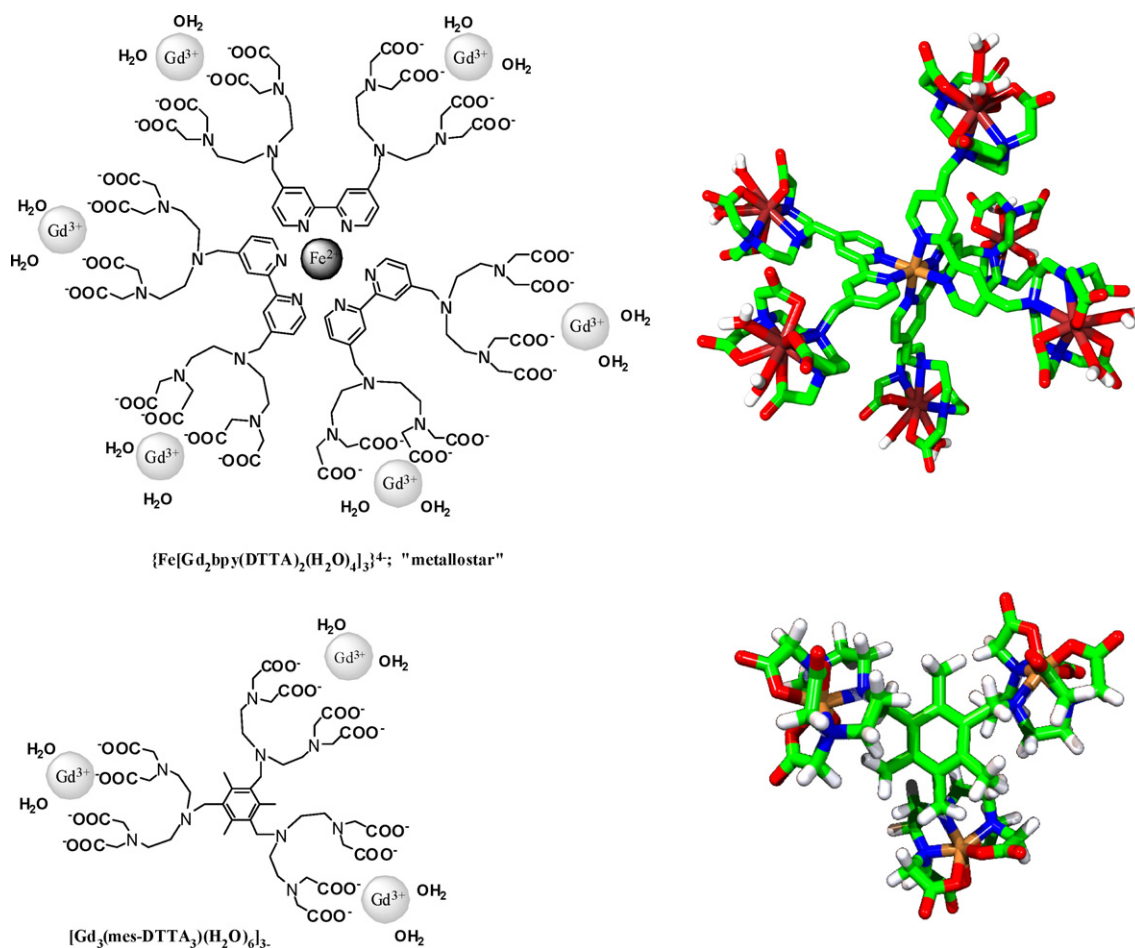


Fig. 2. Variation of the inner-sphere proton relaxivity as a function of the proton Larmor frequency for varying values of the rotational correlation time, τ_R . The curves were calculated for a monohydrated Gd³⁺ complex using the Solomon-Bloembergen-Morgan theory with a water exchange rate of $k_{\text{ex}} = 1 \times 10^7 \text{ s}^{-1}$ and typical values of the electron spin relaxation parameters ($\tau_v = 20 \text{ ps}$, $\Delta^2 = 0.1 \times 10^{20} \text{ s}^{-2}$).



Scheme 3. Examples of "medium-sized" complexes adapted for contrast agent applications at high magnetic field.

emerging domain, and only few dedicated agents have been described.

One of the first examples was an iron-core metallostar, based on the heterotritopic ligand, H₈bpy(DTTA)₂ (Scheme 3) [28]. This ligand has a 2,2'-bipyridine moiety for specific Fe²⁺, and two poly(amino carboxylates) for Gd³⁺-binding. In the presence of Fe²⁺ and Gd³⁺, the system self-assembles to a metallostar {Fe[Gd₂bpy(DTTA)₂(H₂O)₄]₃}⁴⁻ structure (Scheme 3) (metallostars are by definition first-generation metallodendrimers [29]). More recently, a similar structure was constructed by self-assembly around the Ru²⁺ ion, possessing very similar relaxation properties as the Fe²⁺-based analogue [30]. The rational design of H₈bpy(DTTA)₂ involved several key features: (i) The appropriate choice of the lanthanide-chelating poly(amino carboxylate) unit ensures two inner-sphere water molecules to double the inner-sphere contribution to relaxivity and sufficient thermodynamic stability for the Gd³⁺ complex, important for *in vivo* safety. Although the complex stability does decrease [24] with respect to GdDTPA²⁻ where five carboxylate groups of the ligand are coordinated to the lanthanide, it is still sufficient for *in vivo* applications, as was demonstrated in MRI studies in mice [31] (the thermodynamic stability constants are logK_{ML} = 18.2 and 22.5 for the metallostar and

GdDTPA²⁻, respectively [24]). Furthermore, the presence of the two inner-sphere water molecules also guarantees that the water exchange is faster, thus closer to the optimal value than that reported for commercial agents [24]. (ii) Fe²⁺ can accommodate three strongly coordinating 2,2'-bipyridine units which increases to six the number of Gd³⁺ centers on one iron core. The negative charge of {Fe[Gd₂bpy(DTTA)₂(H₂O)₄]₃}⁴⁻ is favorable for high water solubility. (iii) The short linkage between the Fe²⁺ and Gd³⁺ binding sites minimizes internal flexibility that could reduce the relaxivity gain achieved by the increased molecular size. Indeed, the analysis of the rotational dynamics of the metallostar in terms of global and local motions by using the Lipari-Szabo approach proved very limited internal flexibility, most likely originating from the methylene group that links the Fe²⁺ and Gd³⁺ coordinating parts of the ligand [24]. Despite this residual flexibility, the metallostar has a remarkable molar proton relaxivity at all fields. At intermediate fields, its relaxivity is comparable to that of a GdDOTA-loaded Generation 10 dendrimer (27.0 and 33.2 mM⁻¹ s⁻¹ at 25 °C for {Fe[Gd₂bpy(DTTA)₂(H₂O)₄]₃}⁴⁻ vs. 36 and 27 mM⁻¹ s⁻¹ at 23 °C for G10 dendrimer; at 20 and 60 MHz, respectively) [32]. Given its moderate size, the metallostar is a particularly efficient contrast agent at

Table 1
High field relaxivities, r_1 , and molecular weight, M_w , of selected Gd^{3+} complexes.

$r_1/\text{mM}^{-1}\text{s}^{-1}$	200 MHz		400 MHz		M_w	Ref.
	25 °C	37 °C	25 °C	37 °C		
$[\text{Gd}_3(\text{mes-DTTA}_3)(\text{H}_2\text{O})_6]^{3-}$	17.0	14.1	10.7	10.2	1639	[33]
$\{\text{Fe}[\text{Gd}_2\text{bpy}(\text{DTTA})_2(\text{H}_2\text{O})_4]_3\}^{4-}$	16.4	15.9	9.32	8.53	3744	[24]
PAMAM-G4- $[\text{Gd}(\text{DOTA-pBn})(\text{H}_2\text{O})]^{-}_{33}$ Generation 4 dendrimer	8.60	8.41	5.02	4.78	45,000	[19]
$[\text{Gd}(\text{DOTA})(\text{H}_2\text{O})]^{-}$	4.02	3.04	3.86	2.95	575	[33]
$[\text{Gd}(\text{DTPA})(\text{H}_2\text{O})]^{2-}$	4.22	3.20	4.06	3.13	563	[33]

very high magnetic fields (> 100 MHz). Table 1 compares the high field relaxivities of the metallostar to those of the commercial contrast agents GdDTPA^{2-} and GdDOTA^- , as well as of a dendrimeric contrast agent with a large molecular weight. We should also mention that the presence of six efficiently relaxing Gd^{3+} ions within one metallostar leads to an exceptionally high relaxivity confined to a small molecular space (high density of relaxivity).

Another example of a medium-size molecule developed as a high field contrast agent is the trimethylbenzene-core tris- Gd^{3+} complex, $[\text{Gd}_3(\text{mes-DTTA}_3)(\text{H}_2\text{O})_6]^{3-}$ (Scheme 3) [33]. Its Gd^{3+} chelating unit (DTTA^{4-}) is identical to that in the metallostar, allowing for two inner-sphere water molecules and fast water exchange. The 1,3,5-trimethylbenzene core was chosen to maximize rigidity of the molecule. It is interesting to note that as the result of the smaller size with respect to the metallostar $\{\text{Fe}[\text{Gd}_2\text{bpy}(\text{DTTA})_2(\text{H}_2\text{O})_4]_3\}^{4-}$, $[\text{Gd}_3(\text{mes-DTTA}_3)(\text{H}_2\text{O})_6]^{3-}$ has a higher relaxivity at 9.4 T (Table 1).

MRI experiments have been performed with the metallostar at 4.7 Tesla and with $[\text{Gd}_3(\text{mes-DTTA}_3)(\text{H}_2\text{O})_6]^{3-}$ at 9.4 Tesla in mice and compared to the commercial contrast agent GdDOTA^- [31,34]. Both the metallostar and $[\text{Gd}_3(\text{mes-DTTA}_3)(\text{H}_2\text{O})_6]^{3-}$ were well tolerated by the animals at the dose of $8\ \mu\text{mol Gd/kg}$ body weight, despite their bishydrated nature and the resulting slower stability in comparison to GdDOTA^- . Dynamic Contrast Enhanced (DCE) images showed con-

siderably higher signal enhancement in the kidney medulla and cortex after the injection of the high field agents than after GdDOTA^- injection at an identical dose (Fig. 3). These studies have confirmed that the approximately three to four times higher relaxivity (depending on the field) measured *in vitro* for the metallostar or $[\text{Gd}_3(\text{mes-DTTA}_3)(\text{H}_2\text{O})_6]^{3-}$ with respect to GdDOTA^- is retained under *in vivo* conditions. The pharmacokinetics was found to be similar to that of GdDOTA^- , involving fast renal clearance, a leakage to the extracellular space in the muscle tissue and no leakage to the brain.

3. Molecular imaging probes

The objective of molecular imaging is the non invasive *in vivo* investigation of molecular events at the cellular level that might be involved in normal or pathologic processes. Molecular imaging enables the visualization of cellular function and the follow-up of the molecular process in living organisms without perturbing them. Therefore it differs from traditional imaging in that specific molecular imaging probes are used to image particular targets or pathways. Here we will show two specific fields of development of molecular imaging probes. The first aims at the real-time monitoring of calcium concentration changes in the brain, related to neural activity. The second research field concerns the development of contrast agents designed to selectively detect enzyme activity.

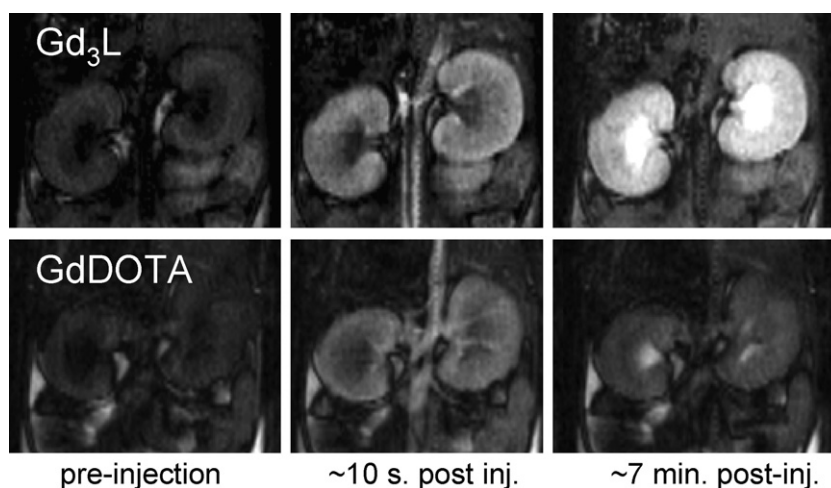


Fig. 3. 9.4 T DCE images of mice kidneys at different times after injection of $[\text{Gd}_3(\text{mes-DTTA}_3)(\text{H}_2\text{O})_6]^{3-}$ (top) and GdDOTA^- (bottom) (both $8\ \mu\text{mol Gd/kg}$ body weight).

3.1. Ca-sensitive agents

Ca^{2+} plays a central role in the physiology and biochemistry of organisms and the cell. It is particularly important in signal transduction pathways, in neurotransmitter release from neurons, contraction of all muscle cell types, and fertilization. Calcium is a cofactor in several enzymes. Ninety-nine percent of the total calcium content in the body is found in the bone and cartilage, the rest is present in the extracellular and intracellular fluids. In a typical cell, the intracellular concentration of ionized calcium is roughly 100 nM, but can increase up to 10–100 fold during certain cellular functions. The Ca^{2+} concentration in extracellular fluids is orders of magnitude higher than the intracellular concentration; in mammalian body fluids, it is around 1.25 mM with minor variations [35].

Our current understanding of the biological role of Ca^{2+} is largely based on optical microscopy techniques using fluorescent dyes capable of measuring Ca^{2+} concentration [36,37]. The limitations of light-based microscopic imaging, involving limited tissue penetration ($\sim 10 \mu\text{m}$) due to light scattering, and the toxicity problems related to the photobleaching byproducts restrict their application to cellular imaging. Given its excellent resolution and unlimited depth penetration, MRI is a viable alternative to optical methods to non-invasive measurement of calcium, provided that adapted calcium-sensitive probes are available.

The real-time visualisation of Ca^{2+} concentration changes by imaging techniques would be particularly interesting to assess neuronal signalling in the brain where Ca^{2+} acts as an important second messenger [38]. Significant changes in Ca^{2+} concentration take place during neuronal activity [39]. The current *in vivo* neuroimaging techniques to follow brain activity are based on blood-oxygen-level dependent (BOLD) functional MRI (fMRI), which has physiological limitations [40], including slow response. Ca^{2+} could be an excellent biomarker for tracking neural activity as it almost instantly enters neurons when they fire and thus it can provide a direct measure of neural activity.

Except for a single calcium-sensitive contrast agent derived from iron-oxide nanoparticles [41], all attempts to create MRI probes for calcium detection are based on Gd^{3+} complexes that generate a Ca^{2+} -dependent relaxivity response. The molecular design involves changes in the coordination sphere of the Gd^{3+} ion following coordination of Ca^{2+} . The probes integrate two binding sites that can selectively coordinate Gd^{3+} and Ca^{2+} ions. These two binding sites are in close proximity, which ensures the coordination of one or more donor groups of the calcium binding site to the Gd^{3+} ion when Ca^{2+} is not present, as depicted in Fig. 4. Upon interaction with Ca^{2+} , this donor group will decoordinate from Gd^{3+} to participate in the Ca^{2+} binding which liberates one coordination position around the Gd^{3+} ion. This coordination position, becoming free around the Gd^{3+} , will be immediately occupied by a water molecule and the increase of the hydration number results in a relaxivity increase. This approach represents the most widely used strategy to create Gd-based MRI contrast agents with a relaxivity response not only to calcium, but also to various metal ions, including copper or zinc [42]. The two main criteria in developing metal responsive imaging probes are that: (i) the probe is responsive to the desired ion in the physiologically relevant concentration range; and (ii) it shows a good selectivity for the metal ion to sense. Both of these aspects are inherently related to the coordination chemistry of the sensed metal ion.

Based on the above concept, a series of dimeric Gd^{3+} complexes have been reported with a specific calcium binding site in the linker between the two macrocyclic Gd^{3+} chelators. GdDOPTA **1**, described by Li et al. [43] 10 years ago, is among the very first examples of molecular imaging agents. The two macrocyclic subunits of the dimeric ligand DOPTA serve as lanthanide(III) ion chelators, while the BAPTA $^{4-}$ subunit bridging the macrocycles is known for its high selectivity towards Ca^{2+} . Indeed, BAPTA $^{4-}$ is a well-known selective fluorescent indicator for Ca^{2+} [44]. The mechanism for the Ca^{2+} -dependent relaxivity change of GdDOPTA has been established through a combined luminescence lifetime and proton relaxation study performed on the Tb^{3+} and Gd^{3+} com-

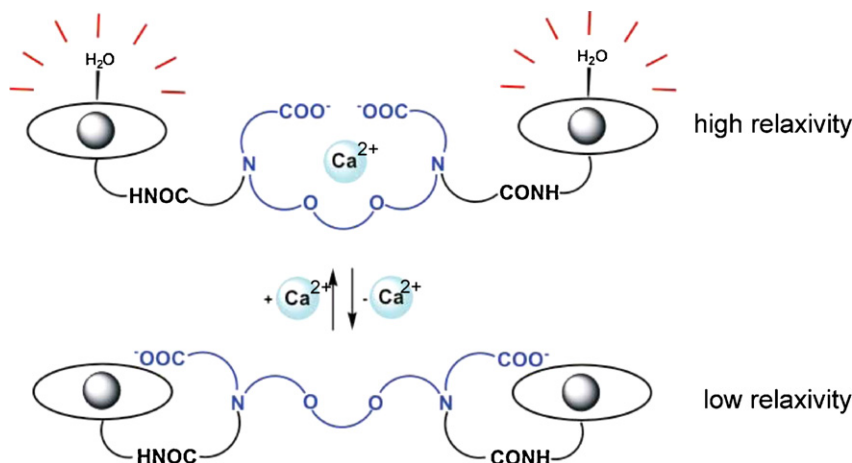
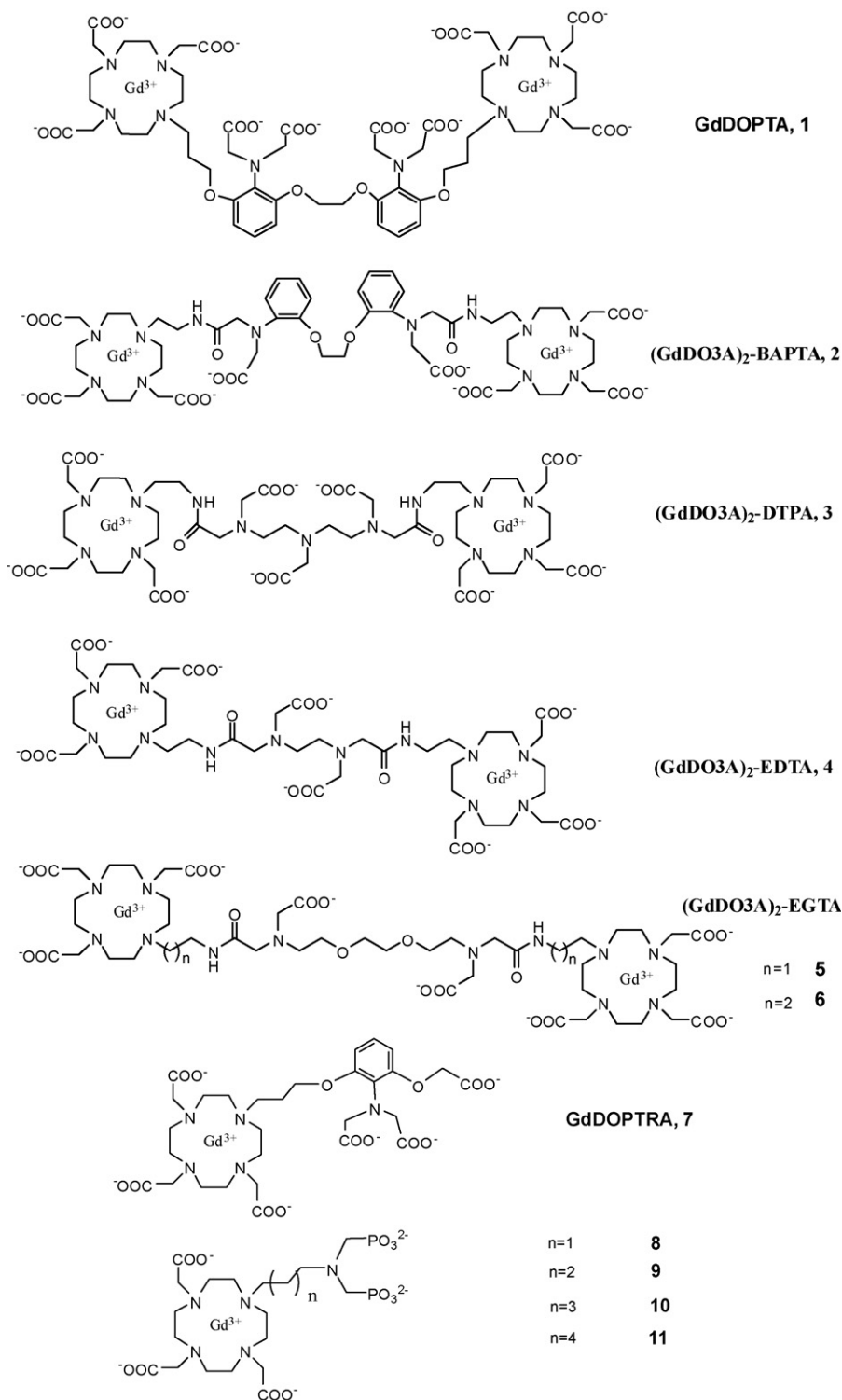


Fig. 4. Illustration of the main strategy to modulate relaxivity of Gd^{3+} complexes by Ca^{2+} recognition.

plexes of DOPTA, respectively [45]. The luminescence lifetime measurements showed that the most important factor responsible of the relaxivity response is the increase in the number of inner-sphere water molecules upon

increasing the Ca^{2+} concentration. GdDOPTA responds to Ca^{2+} in the micromolar range, corresponding to intracellular concentrations. The intracellular delivery of the agent is not evident; moreover, given the low relaxivity of the



Scheme 4. Structure of Gd-based Ca-sensitive contrast agents.

complex, it is not MRI detectable at micromolar concentrations which would be needed to sense Ca^{2+} in the micromolar range. In general, the free extracellular Ca^{2+} concentration, which is in the low millimolar range, can be much more accessible to MRI detection. The extracellular Ca^{2+} concentration also varies significantly during neural stimulation: it drops up to 30–35% from the resting state (typically from 1.2 to 0.8 mM) [46]. Sensing Ca^{2+} changes at millimolar concentrations is more compatible with the relatively high concentrations of the magnetic imaging probe needed to detect contrast changes. In addition, it does not require cell internalization of the imaging probe.

We have reported a series of Gd^{3+} complexes for extracellular Ca^{2+} sensing **2–11** (Scheme 4) [47–49]. In these systems, the two Gd^{3+} -loaded 1,4,7,10-tetraazacyclododecane-1,4,7-triacetic acid (DO3A) units were connected by a BAPTA-, EGTA-, DTPA- or EDTA-derived linker designed for Ca^{2+} binding. In order to create probes adapted to the extracellular calcium concentration, thus with a relaxivity response in the millimolar Ca^{2+} concentration range, these molecules possess a Ca^{2+} binding moiety with reduced affinity towards Ca^{2+} , as compared to BAPTA^{4-} . For instance, in compound **2**, the BAPTA^{4-} ligand was modified by replacing two carboxylates by the less strong donor amide functions. Likewise, bisamide derivatives of DTPA, EDTA or EGTA have been incorporated in ligands **3–6** in order to achieve Ca^{2+} affinity in the millimolar range (Scheme 4). Unfortunately, most of these Gd^{3+} complexes showed limited relaxivity increase (between 10–35%) upon Ca^{2+} binding, with the exception of the EGTA-derivatives **5** and **6** expressing a maximum of 70–80% relaxivity change. The conditional affinity constants for the Ca^{2+} interaction have been determined from relaxometric titrations. As expected, most of them are in the millimolar range, adapted for the assessment of the extracellular Ca^{2+} concentration. The BAPTA- and EGTA-derivative complexes are highly selective toward Ca^{2+} versus Mg^{2+} , which are the only physiologically abundant alkaline earth cations. Not surprisingly, the EDTA- and DTPA-derivatives show much less selectivity towards Ca^{2+} with respect to Mg^{2+} .

On most of these systems, we have performed combined ^{17}O NMR and proton relaxivity studies involving the Gd^{3+} complexes and luminescence measurements on the corresponding Eu^{3+} analogues, both in the absence and presence of Ca^{2+} . The results evidenced that the relaxivity increase observed upon Ca^{2+} addition can be ascribed to the increase in the hydration number, q , and in some cases, to a slight rigidification of the complex resulting from Ca^{2+} binding. In order to simulate the biochemical complexity of the brain, the relaxivity response of **5–6** has been also monitored in a DMEM/F-12/N-2 mixture which is considered as a good mimic of the brain extracellular medium. The relaxivity changes were less important than in water, mounting to ~10% in the relevant range of Ca^{2+} modulation in the brain (0.8–1.2 mM). Although based on these data, complexes **5–6** might be promising for tracking *in vivo* Ca^{2+} concentration changes, the feasibility of such experiments remains to be proved.

Higher relaxivity increase (around 100%) has been recently reported by Dhingra et al. for a monomeric Ca^{2+}

sensitive contrast agent, Gd-DOPTRA, **7** (Scheme 4) [50]. The agent has a great Ca^{2+} selectivity in the presence of Mg^{2+} and Zn^{2+} . In the physiologically more relevant artificial cerebro spinal fluid and artificial extracellular matrix the relaxivity changes on Ca^{2+} binding were also as high as 36 and 25%, respectively. Anion binding was suggested to be responsible for the relaxivity decrease in biological media as compared to water. The affinity constant for Ca^{2+} , as determined by the paramagnetic relaxation enhancement method, is $\sim 9 \times 10^4 \text{ M}^{-1}$. Again, the relaxivity enhancement was mainly attributed to an increase of the hydration number of the Gd^{3+} upon calcium binding.

We have studied DO3A-based complexes bearing an alkyl-aminobis(methylenephosphonate) side chain for Ca^{2+} -chelation (alkyl = propyl (**8**), butyl (**9**), pentyl (**10**) and hexyl (**11**), Scheme 4) [51]. In contrast to all previous calcium-sensitive probes, here the relaxivity of the Gd^{3+} complexes decreases upon addition of Ca^{2+} ; up to ~60% of the initial value for the best compounds **10** and **11**. For these bisphosphonates, the mechanism underlying the calcium-induced relaxivity decrease is relatively complex and not easy to control. It involves aggregation phenomena which operate also in the absence of calcium, and become more important when Ca^{2+} is present. Luminescence lifetime measurements performed on the corresponding Eu^{3+} complexes proved that aggregation reduces the hydration number which is then the main cause of the relaxivity decrease of the Gd^{3+} analogues upon Ca^{2+} binding.

3.2. Enzymatic imaging probes

Enzyme targeting has specific advantages among all molecular imaging agents. An enzyme present at a low concentration can catalytically convert a relatively high amount of the enzyme-responsive probe, which markedly decreases the detection limit for the enzyme as compared to other biomolecules. This can be particularly important when MRI detection is concerned, which typically requires high amounts of the imaging probe. In addition, enzymatic reactions are highly specific; hence the attribution of the observed change in the MR image to a targeted enzyme is straightforward. The overexpression of certain enzymes is often related to pathological conditions. Therefore, the real-time, non-invasive, *in vivo* detection of specific enzymatic activities would have invaluable diagnostic impact. For instance, the importance of specific enzymatic activities has been established in the processes of tumour formation, growth and metastasis. Molecular biology studies have defined enzymatic steps of the apoptotic response to anti-cancer therapies *in vitro* and *in vivo*. On the other hand, the detection of gene markers (such as β -gal) could be also an important field of application of enzyme-responsive MRI probes.

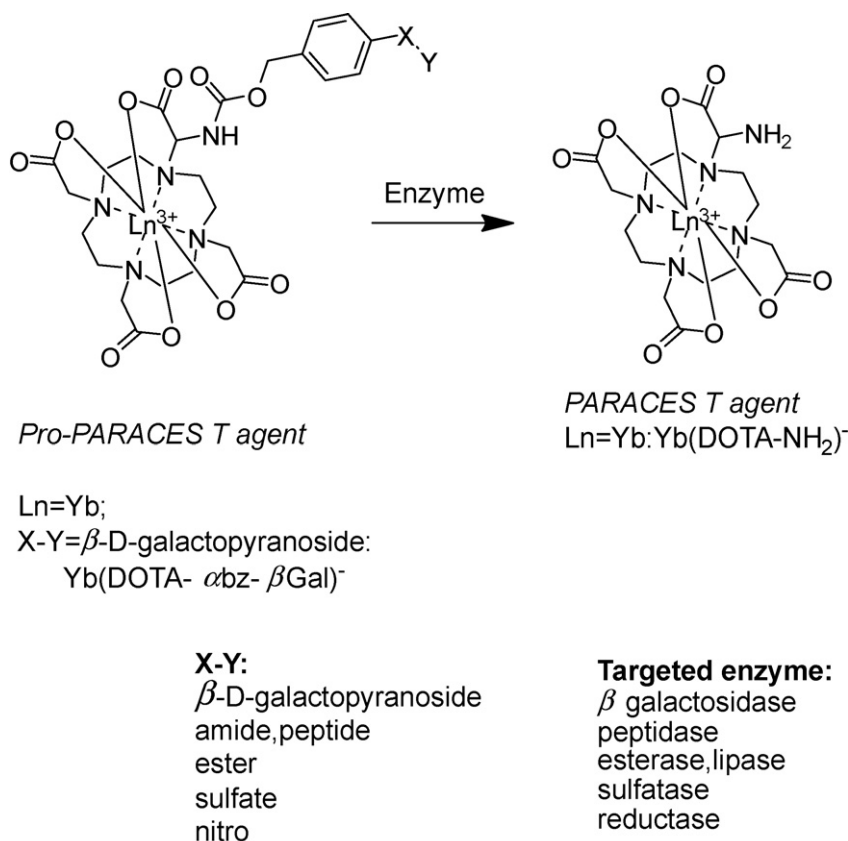
The first enzymatically responsive potential MRI contrast agent was a Gd(DOTA)-derivative bearing a galactopyranose residue that prevents water coordination [52,53]. This sugar moiety is a substrate for the enzyme β -galactosidase. Its enzymatic cleavage by β -galactosidase opens the access of water to the first coordination sphere of

Gd^{3+} , resulting in a relaxivity increase, thus activating the agent in an irreversible way. It has been successfully used for the *in vivo* detection of β -galactosidase mRNA expression in living *Xenopus laevis* embryos. Since this pioneering work of Meade, many examples of enzyme-responsive MRI probes have been reported in the literature. They are based on various mechanisms to modulate the relaxivity of the Gd^{3+} complex upon enzymatic reaction, most often including changes in the size, and thus the rotational motion of the chelate. Among the many examples, the polymerization process was used in several cases to follow the activity of enzymes such as peroxidases [54–58]. McMurry et al. reported the enzymatic transformation of a prodrug Gd^{3+} complex with poor affinity to human serum albumin and low relaxivity, to a species with improved HSA affinity and enhanced relaxivity [59]. In this approach, the origin of the relaxivity increase was the slower rotation for protein-bound chelate with respect to the small molecular weight prodrug. The degradation of a macromolecular Gd^{3+} conjugate could be also used for enzyme detection. A conjugate of a GdDTPA-derivative with hyaluronan, a high molecular weight polysaccharide present in the extracellular matrix, was studied to follow hyaluronidase activity [60,61].

Besides the classical Gd^{3+} -based agents, PARACEST probes with a response to enzymatic activity have also been reported. PARACEST probes represent a new class of potential paramagnetic MRI contrast agents, based on

chemical exchange saturation transfer (CEST) [6,62–65]. PARACEST (Paramagnetic CEST) agents are complexes of lanthanide ions other than gadolinium which possess paramagnetically shifted exchangeable protons. Those protons ($-NH$ of amides, amines or $-OH$ of coordinated water or alcohols) are in slow exchange with bulk water protons (Fig. 1b). They can be selectively saturated by radiofrequency pulses applied at the appropriate frequency, and due to the chemical exchange between these and the water protons, their saturation will result in a decrease of the water proton signal intensity, which becomes observable on an MR image. PARACEST sensors can be based on modulation of the exchange rate or the resonance frequency of those mobile protons on the agent. One advantage of the PARACEST probes with respect to Gd^{3+} -based MRI agents is that the contrast can be switched on and off at will by simply adjusting the pulse sequence parameters. Moreover, PARACEST agents can be also easily adapted to ratiometric approaches that eliminate the problem of an unknown local concentration of the agent. As an enzymatic PARACEST probe, Pagel et al. used a TmDOTA-monoamide complex containing a peptide chain, which is hydrolyzed by the Caspase-3 enzyme [66,67]. Following enzymatic cleavage, the PARACEST effect originating from the amide proton disappears due to the hydrolysis of the amide bond.

We have recently developed a versatile platform of PARACEST agents designed for specific detection of a wide



Scheme 5. Schematic representation of the enzyme-specific platform.

variety of enzymes (Scheme 5) [68]. The molecular design is based on coupling an enzyme-specific substrate to a lanthanide-chelating unit *via* a self-immolative spacer. After enzymatic cleavage of the substrate, the spacer is spontaneously eliminated which results in a concomitant change in the PARACEST properties of the Ln^{3+} chelate. In contrast to the previous enzyme-responsive agents, this platform has the promise of being general and opening the way to specifically target a large variety of enzyme activities. While the Ln^{3+} chelating unit and the self-immolative spacer can be identical for the entire family, the appropriate choice of the substrate will ensure enzyme specificity (Scheme 5). The concept of self-immolative units has been previously proved useful in antibody or gene-directed enzyme prodrug therapy [69–72]. Self-immolative units are often derived from benzyloxycarbamates which are intrinsically instable when possessing an electron donor substituent in *ortho* or *para* position. Based on benzyloxycarbamates as the self-immolative unit, the substrate can be any enzyme-recognized moiety capable of transitionally reducing the electron donor capabilities of the phenyl substituent. The enzymatic cleavage of the substrate initiates an electron cascade and leads to the spontaneous elimination of the spacer. In our system, the self-immolative arm bearing the enzyme-specific substrate is linked to one of the acetate arms of a LnDOTA unit *via* an α carbamoyl nitrogen. The complex $\text{Yb}(\text{DOTA-}\alpha\text{bz-}\beta\text{Gal})^-$ (Scheme 5) has been designed to respond to the activity of β -galactosidase, a commonly used indicator of gene expression. Following the enzymatic attack and the self-immolative electronic cascade, the carbamate is cleaved and transformed to an amine. This results in the appearance of a PARACEST effect attributed to the exchange of the amine protons, while no PARACEST effect is detectable for the carbamate proton of $\text{Yb}(\text{DOTA-}\alpha\text{bz-}\beta\text{Gal})^-$. Typically, amine protons undergo fast exchange, which would not be expected to lead to an observable PARACEST effect. However, the coordination of the adjacent carboxylate and the macrocyclic amine to the lanthanide provides peculiar properties to the exocyclic NH_2 . For instance, its protonation constant, determined by pH-potentiometry for $\text{Gd}(\text{DOTA-NH}_2)^-$, is 4 orders of magnitude lower ($\log K_{\text{H}} = 5.12$) than those for typical amines. Thus the amine in $\text{Yb}(\text{DOTA-NH}_2)^-$ is not protonated at $\text{pH} > 7$ which is likely responsible for the slow proton exchange.

This family of molecular imaging agents possesses several advantages. The substrate is at the extremity of a spacer, thus it does not hinder the enzymatic cleavage. Since the PARACEST effect is observed after enzymatic reaction, it can be optimized once for the whole family and the PARACEST properties will not be affected by the variation of the substrate. Finally, the system works as a switch *off*–*on* probe, which can be a further advantage in practical *in vivo* or *in vitro* applications. We should emphasize the importance of platforms in the development of molecular imaging agents. By nature, molecular imaging probes are unique as they have to be specific to a given target. In most of the time, this requires the development of specialized synthetic schemes to produce each unique MRI contrast agent. The progress in molecular

imaging could be largely accelerated by using platforms where the probes can be adapted to different targets by a small structural modification, without influence on the MRI reporting properties.

4. Bimodal probes

Today, clinical diagnostics and biomedical research dispose of a variety of powerful *in vivo* imaging techniques, including confocal and two-photon microscopy, MRI, positron emission tomography (PET), single photon emission computed tomography (SPECT), or ultrasound. Each of them possesses unique strengths and weaknesses with varying spatial and temporal resolution and sensitivity limits, and therefore they often provide complementary information. Certain dual-modality instruments, such as PET/CT, already have appeared in the clinic [73]. MRI has excellent resolution, though low sensitivity requiring millimolar concentrations of the commercial Gd-based contrast agents for efficient detection. Radioactive tracers and optical imaging probes are orders of magnitude more sensitive and can be detected at much lower concentrations (picomolar or micromolar for PET or optical agents, respectively). In order to combine the advantages of MRI with the benefits of other imaging techniques, there has been an increasing interest in the development of multimodal imaging agents, integrating in a single molecular entity the requirements for MRI and another imaging modality [74]. Such bimodal probes ensure the colocalization of the images acquired by the two modalities and provide a powerful way to an easier interpretation and validation of *in vivo* molecular imaging experiments.

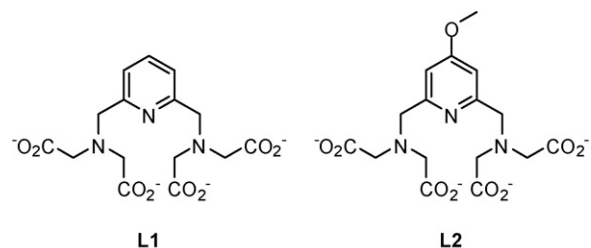
MRI and optical bimodal imaging combine the great spatial, temporal resolution and unlimited tissue penetration of MRI with the sensitivity of the optical imaging probes. The utility of bimodal MRI and optical probes has been proved already in the very first examples of multimodal imaging animal experiments. For instance, Modo et al. used a gadolinium-rhodamine-dextran (GRID) agent to validate by fluorescence microscopy that tracking of transplanted stem cells in rat brain was possible by MRI [75]. Indeed, the distribution of GRID-labeled stem cells identified by *ex vivo* MRI corresponded to those detected using fluorescence microscopy. These results demonstrated that GRID-enhanced MRI can reliably identify transplanted stem cells and their migration in the brain. In the last years, several examples of bimodal agents have been reported, in majority these were Gd^{3+} complexes or iron-oxide nanoparticles combined to organic dyes or quantum dots [76–78].

Lanthanide complexes are particularly well suited for the design of bimodal agents for MRI and optical imaging. Their unique electronic configuration gives them exceptional and varying magnetic and optical properties, while having similar chemical behaviour. Consequently, the replacement of one lanthanide by another will lead to compounds with different physical properties but without major chemical differences. The advantage of using Gd^{3+} complexes as contrast agents for MRI has been largely demonstrated. Moreover, all the Ln^{3+} , except La^{3+} and Lu^{3+} , have potential luminescent properties, some of them being

more efficient than others. Eu^{3+} and Tb^{3+} emit in the visible range, whereas other cations such as Nd^{3+} , Yb^{3+} emit in the near infra-red (NIR) range [79]. The main advantages of using lanthanide complexes as luminescent probes instead of organic compounds include [80]: (a) resistance to photobleaching; (b) long-lived excited state allowing the short-lived biological background fluorescence to disperse before the lanthanide emission occurs; (c) absence of reabsorption; and (d) line-like emission bands, whose wavelengths are characteristic of the lanthanide only (negligible influence of the ligand). Unfortunately the direct excitation of lanthanide is not easily achieved as f-f transitions are forbidden. However, this problem can be solved *via* indirect excitation by a sensitized chromophore using the so-called “antenna effect”. The excited antenna will pass its energy to the excited state of the lanthanide, which can emit light. The requirements to meet for an efficient energy transfer are: (i) choose a suitable chromophore (excited energy level adapted to the excited state of the lanthanide); and (ii) have an optimized distance between the chromophore and the lanthanide ion [81]. Another important point in the design of an efficient lanthanide-based probe is to protect the lanthanide cation from solvent molecules, and particularly water. Indeed, lanthanide emission is quenched by the presence of water molecules in the first coordination sphere of the lanthanide (non-radiative deactivation through O-H vibrators). Lanthanide ions that emit in the NIR range have commonly lower quantum yield than those emitting in the visible range but they are more suitable for biological applications as they can be excited at lower energy and NIR photons can go deeper into tissue.

Despite these positive features of lanthanides, reports on Ln^{3+} complexes using an identical ligand structure to create combined MRI and optical probes have been rather scarce [82–87], and as far as MRI – NIR luminescent agents are concerned, there are only two reports in the literature [88,89]. The main reason is that the design of efficient bimodal probes is a real challenge for the coordination chemist: while the presence of at least one inner-sphere water molecule is required for a good MRI efficiency, water molecules in the proximity of the lanthanide ion are undesired for optical purposes since they strongly quench the luminescence. Indeed, the combined requirements for both imaging techniques were often considered to be non-compatible.

We have recently reported on a versatile pyridine-based scaffold for Ln^{3+} complexation where MRI and luminescence requirements are simultaneously satisfied using the same ligand (Scheme 6) [89]. It has been shown that the lanthanide ion is bishydrated, giving rise to a good MRI efficacy in the case of the Gd^{3+} complex ($r_1 = 6.21 \text{ mM}^{-1} \text{ s}^{-1}$ at 500 MHz and 25 °C for GdL1). Surprisingly, the pyridine acts as a very efficient sensitizer of the corresponding Nd^{3+} complex through the “antenna effect” and can compensate for the quenching caused by the two inner-sphere waters. It has been demonstrated for the first time that the presence of two water molecules bound to the lanthanide cation is not an absolute limitation for the development of NIR luminescent compounds. The quantum yield measured for the bishy-



Scheme 6. Structure of the bimodal probes.

drated Nd^{3+} complex is remarkable for a NIR emitting lanthanide (0.0097% for NdL1 in H_2O), and falls in the same range as the non-hydrated system so far best optimized for aqueous NIR applications (0.027% in H_2O) [90]. The thermodynamic stability and the dissociation kinetic properties of these pyridine-based lanthanide complexes also have been studied. The thermodynamic stability is high for a bishydrated complex ($\log K_{\text{GdL}} \sim 18.6$), and the selectivity of the ligand for lanthanides over endogenous cations such as Ca^{2+} , Zn^{2+} , Cu^{2+} is also very good. Moreover, GdL1 was found to be kinetically more inert than the commercial contrast agent GdDTPA^{2-} . Toxicity assays in various cell lines and mice showed no toxicity of these complexes. Finally, another important parameter for *in vivo* study is the formation of ternary complexes with endogenous anions. These anions can replace the water molecules in the first coordination sphere leading to dramatic decrease of the relaxivity. Importantly, the lanthanide complexes of the pyridine-based ligands have no tendency to form ternary complexes with anions such as carbonate or phosphate. The emission spectra of EuL1 recorded in pure water and in the presence of 600 equivalents of carbonate or phosphate (pH 7.4) were identical, excluding the formation of ternary complex. These results are promising and we are currently working on derivatives of such ligands with an increased conjugation of the pyridine in order to lower the excitation energy of the corresponding NIR complexes and optimize both MRI and luminescent properties. This versatile pyridine-based platform offers numerous possibilities of optimization and combination to biological vectors, and might have a potential use in bimodal imaging (MRI and NIR) based on lanthanide complexes. Evidently, bimodal probes have to account for the differences in sensitivity of the imaging modality. The MRI reporter Gd^{3+} complex has to be administered in at least ~ 100 fold higher concentration than the luminescent optical probe.

Recently, the same pyridine-based platform was used in an approach proposed for the rapid screening of chromophores for lanthanide sensitization. In order to achieve an efficient energy transfer from the chromophore to the lanthanide, the two entities should be in close proximity and this is typically achieved by creating a covalent linkage between the chromophore and the lanthanide complexing unit. This very often requires difficult and time-consuming synthetic procedures and does not automatically result in a compound with a good quantum yield, as the efficiency of the chromophore can be tested only on the final compound. We have proposed to test chromophores by

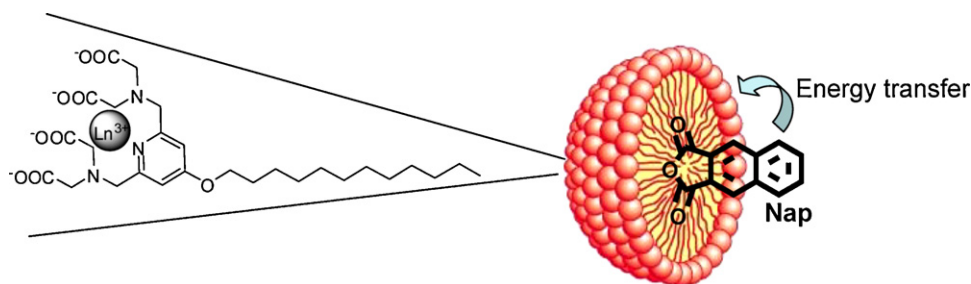


Fig. 5. Schematic representation of the micelle with the inclusion of the chromophore.

including them in a micelle formed by an amphiphilic lanthanide complex when the energy transfer occurs between the two non-covalently linked moieties. The feasibility of the method was illustrated for a naphthalene-derivative chromophore and a pyridine-based lanthanide complex with a C12 hydrophobic chain (Fig. 5) [91]. This simple and rapid approach offers not only a convenient way of screening a variety of hydrophobic chromophores without important synthetic effort, but also the creation of luminescent polymetallic particles with a high number of integrated chromophores and lanthanide cations. In addition, it allows assessing the fate of micelles in biological media. In terms of bimodal probes, the formation of micelle has already been exploited to optimize MRI properties and we have shown that this technique can be used to optimize luminescent intensity also.

5. Conclusions and perspectives

The field of biomedical imaging has been continuously benefiting from the use of lanthanide-based imaging probes, in particular Gd³⁺ chelates, widely applied in MRI. In parallel, this great success promoted considerable interest in lanthanide coordination chemistry. The optimization of the contrast enhancing properties of Gd³⁺ complexes *via* a rational ligand design has been and will likely remain in a central position of contrast agent research. The technical advances in MRI implying the use of high magnetic fields promoted the development of a new class of Gd³⁺-based agents specifically optimized for such high field applications.

The emergence of molecular imaging, seeking for the visualisation of molecular events, opened novel perspectives in the biomedical use of lanthanide complexes. Coordination chemistry offers practically unlimited possibilities to translate the interaction of a metal-based imaging probe with another metal ion, an enzyme, a metabolite, etc. into a magnetic response which ensures a bright future of lanthanide chemistry in the development of molecular imaging approaches.

The combination of two imaging modalities allows for combining the benefits of each technique, which explains the success of bimodal imaging. This calls for bimodal imaging probes that integrate the requirements of the two modalities within a single molecule. Lanthanides, possessing varying magnetic and optical properties but very similar coordination chemistry, are excellent candidates

for the development of bimodal probes for MRI and optical applications.

Acknowledgements

We gratefully acknowledge funding from the CNRS, the National Institute of Cancer, The Cancer Ligue and the National Research Agency (ANR), France, as well as the European COST Action D38 “Metal-Based Systems for Molecular Imaging Applications”. The research efforts of many postgraduate and postdoctoral associates involved in this work are also acknowledged.

References

- [1] A.E. Merbach, É. Tóth (Eds.), *The chemistry of contrast agents in medical magnetic resonance imaging*, Wiley, New York, 2001.
- [2] S. Aime, M. Botta, E. Terreno, *Adv. Inorg. Chem.* 57 (2005) 173.
- [3] C.F.G.C. Geraldes, S. Laurent, *Imaging* 4 (2009) 1.
- [4] V. Kubiček, É. Tóth, *Adv. Inorg. Chem.* 61 (2009) 63.
- [5] D. Parker, R.S. Dickins, H. Puschmann, C. Crossland, J.A.K. Howard, *Chem. Rev.* 102 (2002) 1977.
- [6] M. Woods, D.E. Woessner, A.D. Sherry, *Chem. Soc. Rev.* 35 (2006) 500.
- [7] P. Caravan, *Chem. Soc. Rev.* 35 (2006) 512.
- [8] (a) J.C.G. Bünzli, C. Piguet, *Chem. Soc. Rev.* 34 (2005) 1048; (b) J.C.G. Bünzli, S. Comby, A.S. Chauvin, C.D.B. Vandevyver, *J. Rare Earths* 25 (2007) 257; (c) P. Caravan, J.J. Ellinson, T.J. McMurphy, R.B. Lauffer, *Chem. Rev.* 99 (1999) 2293.
- [9] (a) S. Liu, *Adv. Drug Deliv. Rev.* 60 (2008) 1347; (b) F. Roesch, *Radiochim. Acta* 95 (2007) 303; (c) W.A. Volkert, T.J. Hoffman, *Chem. Rev.* 99 (1999) 2269; (d) S.P. Fricker, *Chem. Soc. Rev.* 35 (2006) 524.
- [10] S. Trattnig, K. Pinker, A. Ba-Ssalamh, I.M. Nöbauer-Huhmann, *Eur. Radiol.* 16 (2006) 1280.
- [11] R.G. Pautler, *Physiology* 19 (2004) 168.
- [12] T. Vaughan, L. DelaBarre, C.C. Snyder, J. Tian, C. Akgun, D. Shrivastava, W. Liu, C. Olson, G. Adirany, J. Strupp, P. Andersen, A. Gopinath, P.F. van de Moortele, M. Garwood, K. Ugurbil, *Mag. Reson. Med.* 56 (2006) 1274.
- [13] P. Védrine, G. Aubert, F. Beaudet, J. Belorgey, J. Beltramelli, C. Berriaud, P. Bredy, P. Chesny, A. Donati, G. Gilgrass, G. Grunblatt, F.P. Juster, F. Molinier, C. Meuris, F. Nunio, A. Payn, L. Quettier, J.M. Rey, T. Schild, A. Sinanna, *IEEE Trans. Appl. Superconduct.* 18 (2008) 868.
- [14] R. Ruloff, É. Tóth, R. Scopelliti, R. Tripier, H. Handle, A.E. Merbach, *Chem. Commun.* 22 (2002) 2630.
- [15] S. Laus, R. Ruloff, É. Tóth, A.E. Merbach, *Chem. Eur. J.* 9 (2003) 3555.
- [16] Z. Pálkás, A. Roca-Sabio, M. Mato-Iglesias, D. Esteban-Gómez, C. Platas-Iglesias, A. de Blas, T. Rodríguez-Blas, É. Tóth, *Inorg. Chem.* 48 (2009) 8878.
- [17] D.M.J. Doble, M. Botta, J. Wang, S. Aime, A. Barge, K.N. Raymond, *J. Am. Chem. Soc.* 123 (2001) 10758.
- [18] L. Tei, G. Gugliotta, Z. Baranyai, M. Botta, *Dalton Trans.* (2009) 9712.
- [19] Z. Jászberényi, L. Moriggi, P. Schmidt, C. Weidensteiner, R. Kneuer, A.E. Merbach, L. Helm, É. Tóth, *J. Biol. Inorg. Chem.* 12 (2007) 406.
- [20] S. Torres, J.P. André, J.A. Martins, C.F.G.C. Geraldes, A.E. Merbach, É. Tóth, *Chem. Eur. J.* 12 (2006) 940.

- [21] P. Caravan, N.J. Cloutier, M.T. Greenfield, S.A. McDermid, S.U. Dunham, J.W.M. Bulte, J.C. Amedio, R.J. Looby Jr., R.M. Supkowski, DeW. Horrocks Jr., T. McMurry, R.B. Lauffer, *J. Am. Chem. Soc.* 124 (2002) 3152.
- [22] A. Datta, K.N. Raymond, *Acc. Chem. Res.* (2009) 938.
- [23] (a) S. Aime, L. Calabi, C. Cavallotti, E. Gianolio, G.B. Giovenzana, P. Losi, A. Maiocchi, G. Palmisano, M. Sisti, *Inorg. Chem.* 43 (2004) 7588; (b) Z. Baranyai, F. Uggeri, G.B. Giovenzana, A. Bényei, E. Brucher, S. Aime, *Chem. Eur. J.* 15 (2009) 1696.
- [24] J.B. Livramento, A. Sour, A. Borel, A.E. Merbach, É. Tóth, *Chem. Eur. J.* 12 (2006) 989.
- [25] S. Aime, M. Botta, S.G. Crich, G.B. Giovenzana, G. Jommi, R. Pagliarin, M. Sisti, *Inorg. Chem.* 36 (1997) 2992.
- [26] C.S. Bonnet, P.H. Fries, S. Crouzy, O. Seneque, F. Cisnetti, D. Boturyn, P. Dumy, P. Delange, *Chem. Eur. J.* 15 (2009) 7083.
- [27] E. Balogh, M. Mato-Iglesias, C. Platas-Iglesias, É. Tóth, K. Djanashvili, J.A. Peters, A. de Blas, T. Rodríguez-Blas, *Inorg. Chem.* 45 (2006) 8719.
- [28] J.B. Livramento, É. Tóth, A. Sour, A. Borel, A.E. Merbach, R. Ruloff, *Angew. Chem. Int. Ed.* 44 (2005) 1480.
- [29] E. Constable, in: *Comprehensive Coordination Chemistry II*, Elsevier Ltd, Oxford, 7 (2004) 263.
- [30] L. Moriggi, A. Aebischer, C. Cannizzo, A. Sour, A. Borel, J.C.G. Bünzli, L. Helm, *Dalton Trans.* (2009) 2088.
- [31] J.B. Livramento, C. Weidensteiner, M.I.M. Prata, P.R. Allegrini, C.F.G.C. Geraldes, L. Helm, R. Kneuer, A.E. Merbach, A.C. Santos, P. Schmidt, É. Tóth, *Contrast Med. Mol. Imaging* 1 (2006) 30.
- [32] L.H. Bryant Jr., M.W. Brechbiel, W. Chuanhua, J.W.M. Bulte, V. Herynek, J.A. Frank, *J. Magn. Reson. Imaging* 9 (1999) 348.
- [33] J.B. Livramento, L. Helm, A. Sour, C. O'Neil, A.E. Merbach, É. Tóth, *Dalton Trans.* (2008) 1195.
- [34] P. Loureiro de Sousa, J.B. Livramento, L. Helm, A.E. Merbach, W. Mème, B.T. Doan, J.C. Beloelil, M.I.M. Prata, A.C. Santos, C.F.G.C. Geraldes, É. Tóth, *Contrast Med. Mol. Imaging* 3 (2008) 78.
- [35] S. Forsen, J. Kordel, in: I. Bertini, H.B. Gray, S.J. Lippard, J.S. Valentine (Eds.), *Calcium in biological systems in bioinorganic chemistry*, University Science Books, Mill Valley, California, 1994, p. 107.
- [36] (a) R.Y. Tsien, A. Waggoner, in: J.B. Pawley (Ed.), *Handbook of biological confocal microscopy*, 2nd ed, Plenum Press, New York, 1995, p. 267; (b) R.Y. Tsien, *Chem. Eng. News* 72 (1994) 34; (c) A.W. Czarnik (Ed.), *ACS Symposium Series 538*, American Chemical Society, Washington, DC, 1993.
- [37] (a) J. Waters, M. Larkum, B. Sakmann, F. Helmchen, *J. Neurosci* 23 (2003) 8558; (b) J.N.D. Kerr, D. Greenberg, F. Helmchen, *Proc. Natl. Acad. Sci. U. S. A.* 102 (2005) 14063; (c) K. Ohki, S. Chung, Y.H. Ch'ng, P. Kara, R.C. Reid, *Nature* 433 (2005) 597.
- [38] R.W. Tsien, R.Y. Tsien, *Annu. Rev. Cell Biol.* 6 (1990) 715.
- [39] J. Meldolesi, *Nature* 392 (1998) 863.
- [40] N.K. Logothetis, *Nature* 453 (2008) 869.
- [41] T. Atanasijevic, M. Shusteff, P. Fam, A. Jasanoff, *Proc. Natl. Acad. Sci. U. S. A.* 103 (2006) 14707.
- [42] C. Bonnet, E. Toth, *Future Med. Chem.* 2010, in press.
- [43] W. Li, S.E. Fraser, T.J. Meade, *J. Am. Chem. Soc.* 121 (1999) 1413.
- [44] R.Y. Tsien, *Biochemistry* 19 (1980) 2396.
- [45] W. Li, G. Parigi, M. Fragai, C. Luchinat, T.J. Meade, *Inorg. Chem.* 41 (2002) 4018.
- [46] D.A. Hammoud, J.M. Hoffman, M.G. Pomer, *Radiology* 245 245 (2007) 21.
- [47] K. Dhingra, P. Fousková, G. Angelovski, M.E. Maier, N.K. Logothetis, E. Toth, *J. Biol. Inorg. Chem.* 13 (2008) 35.
- [48] A. Mishra, P. Fousková, G. Angelovski, E. Balogh, A.K. Mishra, N.K. Logothetis, É. Tóth, *Inorg. Chem.* 47 (2008) 1370.
- [49] G. Angelovski, P. Fousková, I. Mamedov, S. Canals, E. Toth, N.K. Logothetis, *Chem. Bio. Chem.* 9 (2008) 1729.
- [50] K. Dhingra, M.E. Maier, M. Beyerlein, G. Angelovski, N.K. Logothetis, *Chem. Commun* (2008) 3444.
- [51] I. Mamedov, J. Henig, G. Angelovski, P. Fouskova, É. Tóth, N. K. Logothetis, H. A. Mayer, submitted.
- [52] R.A. Moats, S.E. Fraser, T.J. Meade, *Angew. Chem. Int. Ed. Engl.* 36 (1997) 726.
- [53] A.Y. Louie, M.M. Hüber, E.T. Ahrens, U. Rothbächer, R. Moats, R.E. Jacobs, S.E. Fraser, T.J. Meade, *Nat. Biotechnol.* 18 (2000) 321.
- [54] J.W. Chen, W. Pham, R. Weissleder, A. Bogdanov, *Magn. Reson. Med.* 52 (2004) 1021.
- [55] M. Querol, J.W. Chen, R. Weissleder, A. Bogdanov, *Org. Lett.* 7 (2005) 1719.
- [56] J.W. Chen, M. Querol, A. Bogdanov, R. Weissleder *Radiol.* 240 (2006) 473.
- [57] M. Querol, J.W. Chen, A. Bogdanov, *Org. Biomol. Chem.* 4 (2006) 1887.
- [58] M. Querol, D.G. Bennett, C. Sotak, H. Won Kang, A. Bogdanov, *Chem. Bio. Chem.* 8 (2007) 1637.
- [59] A.L. Nivorozhkin, A.F. Kolodziej, P. Caravan, M.T. Greenfield, R.B. Lauffer, T.J. McMurry, *Angew. Chem. Int. Ed. Engl.* 40 (2001) 2903.
- [60] L. Shifftan, T. Israely, M. Cohen, V. Frydman, H. Dafni, R. Stern, M. Neeman, *Cancer Res.* 65 (2005) 10316.
- [61] L. Shifftan, M. Neeman, *Contrast Med. Mol. Imaging* 1 (2006) 106.
- [62] S. Aime, D. Delli Castelli, E. Terreno, *Angew. Chem. Int. Ed.* 41 (2002) 4334.
- [63] S.S. Zhang, P. Winter, K. Wu, A.D. Sherry, *J. Am. Chem. Soc.* 123 (2001) 1517.
- [64] D.E. Woessner, S. Zhang, M.E. Merritt, A.D. Sherry, *Magn. Reson. Med.* 53 (2005) 790.
- [65] A.D. Sherry, M. Woods, *Annu. Rev. Biomed. Eng.* 10 (2008) 391.
- [66] B. Yoo, M.D. Pagel, *J. Am. Chem. Soc.* 128 (2006) 14032.
- [67] B. Yoo, M.S. Raam, R.M. Rosenblum, M.D. Pagel, *Contrast Med. Mol. Imaging* 2 (2007) 189.
- [68] T. Chauvin, P. Durand, M. Bernier, H. Meudal, B.-T. Doan, F. Noury, B. Badet, J.-C. Beloelil, E. Toth, *Angew. Chem. Int. Ed. Engl.* 47 (2008) 4370.
- [69] P.L. Carl, P.K. Chakravarty, J.A. Katzenellenbogen, *J. Med. Chem.* 24 (1981) 479.
- [70] J.L. Guerquin-Kern, A. Olk, E. Chenu, R. Lougerstay-Madec, C. Monneret, J.C. Florent, D. le Carrez, A. Croisy, *NMR Biomed.* 13 (2000) 306.
- [71] R. Madec-Lougerstay, J.C. Florent, C. Monneret, *J. Chem. Soc. Perkin Trans 1* (1999) 1369.
- [72] F.M.H. de Groot, W.J. Loos, R. Koekoek, L.W.A. van Berkum, G.F. Busscher, A.E. Seelen, C. Albrecht, P. de Bruijn, H.W. Scheeren, *J. Org. Chem.* 66 (2001) 8815.
- [73] K. Wechalekar, B. Sharma, G. Cook, *Clin. Radiol.* 60 (2005) 1143.
- [74] (a) L. Frullano, T.J. Meade, *J. Biol. Inorg. Chem.* 12 (2007) 939; (b) W.J.M. Mulder, G.J. Strijkers, R. Koole, C.D.M. Donega, G. Storm, A.W. Griffioen, K. Nicolay, in: *Bimodal liposomes and paramagnetic QD-Micelles for multimodality molecular imaging of tumor angiogenesis in nanoparticles in biomedical imaging*, Springer, New York, 2007.
- [75] M. Modo, D. Cash, K. Mellodew, S.C.R. Williams, S.E. Fraser, T.J. Meade, J. Price, H. Hodges *Neuro. Image* 17 (2002) 803.
- [76] A. Tsourkas, V.R. Shinde-Patil, K.A. Kelly, P. Patel, A. Wolley, J.R. Allport, R. Weissleder, *Bioconjugate Chem.* 16 (2005) 576.
- [77] Y.M. Huh, Y.W. Jun, H.T. Song, S. Kim, J.S. Choi, J.H. Lee, S. Yoon, K.S. Kim, J.S. Shin, J.S. Suh, J. Cheon, *J. Am. Chem. Soc.* 127 (2005) 12387.
- [78] W. Mulder, R. Koole, R. Brandwijk, G. Storm, P.T.K. Chin, G. Strijkers, C. deMelloDonega, K. Nicolay, A. Griffioen, *Nano Lett.* 6 (2006) 1.
- [79] J.-C.G. Bünzli, C. Piguet, *Chem. Soc. Rev.* 34 (2005) 1048.
- [80] C.M.G. dos Santos, A.J. Harte, S.J. Quinn, T. Gunnlaugsson, *Coord. Chem. Rev.* 252 (2008) 2512.
- [81] S.I. Weissman, *J. Chem. Phys.* 10 (1942) 214.
- [82] S. Laurent, L. Vander Elst, M. Wautier, C. Galaup, R.N. Muller, C. Picard, *Bioorg. Med. Chem. Lett.* 17 (2007) 6230.
- [83] S.G. Crich, L. Biancone, V. Cantaluppi, D. Duò, G. Esposito, S. Russo, G. Camussi, S. Aime, *Magn. Reson. Med.* 51 (2004) 938.
- [84] I. Nasso, C. Galaup, F. Havas, P. Tisnès, C. Picard, S. Laurent, L. Vander Elst, R.N. Muller, *Inorg. Chem.* 44 (2005) 8293.
- [85] M.P. Lowe, D. Parker, O. reany, S. Aime, M. Botta, G. Castellano, E. Gianolio, R. Pagliarin, *J. Am. Chem. Soc.* 123 (2001) 7601.
- [86] C. Gunanathan, A. Pais, E. Furman-Haran, D. Seger, E. Eyal, S. Mukhopadhyay, Y. Ben-David, G. Leituss, H. Cohen, A. Vilan, H. Degani, D. Milstein, *Bioconjugate Chem.* 18 (2007) 1361.
- [87] H.C. Manning, T. Goebel, R.C. Thompson, R.R. Price, H. Lee, D.J. Bornhop, *Bioconjugate Chem.* 15 (2004) 1488.
- [88] T. Koullourou, L.S. Natrajan, H. Bhavsar, S.J.A. Pope, J. Feng, J. Narvainen, R. Shaw, E. Scales, R. Kauppinen, A.M. Kenwright, S. Faulkner, *J. Am. Chem. Soc.* 130 (2008) 2178.
- [89] L. Pellegatti, J. Zhang, B. Drahos, S. Villette, F. Suzenet, G. Guillaumet, S. Petoud, É. Tóth, *Chem. Commun* (2008) 6591.
- [90] S. Comby, D. Imbert, C. Vandevyver, J.-C.G. Bünzli, *Chem. Eur. J.* 13 (2007) 936.
- [91] C.S. Bonnet, L. Pellegatti, F. Buron, C.M. Shade, S. Villette, V. Kubicek, G. Guillaumet, F. Suzenet, S. Petoud, É. Tóth, *Chem. Commun* 46 (2010) 124.